USSR ACADEMY OF SCIENCES,
P.N. LEBEDEV INSTITUTE OF PHYSICS (ORDER OF LENIN)

Preprint No. 45

USING A LOW-PRESSURE SPARK CHAMBER TO MEASURE PRIMARY IONIZATION IN GASES

V.S. Asoskov, V.V. Blazhenkov, V.M. Grishin,
L.P. Kotenko, G.I. Merzon, L.S. Pervov

Moscow 1975

Translated at CERN by R. Luther
(Original: Russian)
Not revised by the Translation Service

(CERN Trans. 75-4)

Geneva
July 1975

The possibility of measuring primary specific ionization in pure inert gases in terms of a low-pressure spark chamber's efficiency is demonstrated experimentally. It is found that in a wire spark chamber the effects of electron diffusion during the HV-pulse delay time and of electron drift on to the electrodes are considerably reduced, thus making it possible to carry out precision measurements of the primary ionization even in gases with a high electron diffusion coefficient. Preliminary results from the measurement of the minimum primary specific ionization in helium, neon and argon are given.

The dependence of a spark chamber's efficiency on a particle's ionization potential may be used in order to measure primary specific ionization in gases (1-3) in the same way as is done using low-efficiency Geiger-Müller counters. This obvious idea has not yet been put into practice even though the spark chamber method has potential advantages over other means of measuring primary specific ionization. For instance, unlike low-efficiency counters (4,5) and also the Wilson chamber (6,7) and diffusion cloud chamber (8) where admixtures have to be present in the process gas if the device is to work, the spark chamber allows primary ionization to be measured in pure gases. The spark chamber method is much simpler than the streamer chamber method (9-12) and unlike the latter allows measurements to be carried out even in gases with a high diffusion coefficient, as will be shown below.

It is interesting to measure primary ionization because its relativistic rise may be used to identify high-energy charged particles in the Lorentz factor region $\gamma \lesssim 10^2$ (2. 12). However, primary specific ionization has hitherto been measured only in a small number of gases and over a limited range of γ values. Existing theoretical data on the primary ionization of relativistic particles in gases (13, 14) are lacking in support and require further checking.

In this report it is shown by experiment that it is possible to measure primary specific ionization in terms of a spark chamber's efficiency. A solution is also found to the problems caused by the loss of some of the electrons produced by particles in the gas owing to their diffusion and to the fact that they drift in the HV-pulse's field to the spark chamber electrodes.

1. Primary ionization and spark chamber efficiency

Owing to the random nature of particle collisions in the spark chamber gas, the rate P_j of production of j primary ion pairs is subject to a Poisson distribution with an average value

$$n = \ell\,(dn/dx)_{P,T} = \frac{273}{T} p \ell\,(dn/dx), \qquad (1)$$

where $(dn/dx)_{P,T}\,cm^{-1}$ is the primary specific gas ionization caused by the charged particle at a pressure of P atm and a temperature of T°K, and $(dn/dx)\,cm^{-1}$ is under normal conditions and ℓ cm is the interelectrode gap. If one free electron is enough to generate a spark (the data obtained from streamer chambers (9-12) show that this does happen when the HV pulse rises steeply to a large value), then the spark chamber's efficiency is

$$\eta = 1 - P_0 = 1 - \exp[-\ell\,(dn/dx)_{P,T}]. \qquad (2)$$

The standard error $\langle \Delta \eta \rangle$ of the efficiency measurements may be calculated from the binomial distribution, and after N measurements it amounts to

$$\langle \Delta\eta \rangle = [\eta(1-\eta)/N]^{1/2} \qquad (3)$$

The primary ionization is

$$(dn/dx)_{P,T} = \frac{\ell n(1-\eta)}{\ell}\,, \qquad (4)$$

and its standard deviation is

$$\langle \Delta (dn/dx)_{P,T} \rangle = \frac{1}{\ell} \left\{ \frac{\exp[\ell (dn/dx)_{PT}] - 1}{N} \right\}^{1/2} \qquad (5)$$

The maximum accuracy of the primary ionization measurements corresponds to $\ell (dn/dx)_{P,T} = 1.6$, i.e. $\eta = 0.80$ (15), and this accuracy is 3.9% at $N = 10^3$, although over the range $0.5 < \eta < 0.95$ the standard error varies slightly and does not exceed 4.6% for the same statistics.

If the calculated values of (dn/dx) (13,14) are used, then the primary ionization is best measured at $\ell \simeq 1$ cm when the pressures are below atmospheric pressure (Table 1). It is not advisable to reduce the interelectrode gap (when P is still $\simeq$ 1 atm) because this increases the spark chamber's self-capacitance and worsens the shape of the HV-pulse. Moreover, it becomes more difficult to keep the interelectrode gap at precisely the right value. Low-pressure spark chambers were therefore used for the measurements.

Allowance must be made for the fact that some of the electrons produced by the charged particle in the gas are diffused and also drift in the electric field on the leading edge of the HV-pulse: as a result they strike the electrodes and do not contribute to the spark discharge. Therefore, the ℓ value in expressions (1-5) must be replaced by the effective interelectrode distance $\ell_e < \ell$, the value of which depends on the conditions of the experiment and has to be determined.

2. Experimental device

The layout of one type of experimental device is shown in fig. 1. The electrons produced by the Sr^{90}_{38} beta source with an energy of 1.7 - 2.2 MeV* and an intensity of $\sim 2.10^{-4}$ decay/min

---

* The primary specific ionization produced by these electrons is on average not more than 0.5% from the minimum (13,14).

passed through the control (SC and SC_3) and test (SC_2) spark chambers and were recorded by scintillation counters S_1 and S_2. The S_1S_2 coincidence pulse triggered the spark chambers' power supply circuit consisting of TGI-325/16 thyratrons. Spark chambers SC_1 and SC_3 were filled with neon and were nearly 100% efficient. Test chamber SC_2 was filled with a chemically pure gas containing less than 0.01% admixtures. The gas pressure was checked either by a 0.5 type indicating pressure gauge, or by a mercury pressure gauge (at $P \geqslant 0.5$ atm) or by a U-shaped oil gauge (at $P \leqslant 0.15$ atm). Information about the spark in SC, and SC_3 was recorded by means of ferrite rings, and in SC_2 by means of an FEU-68 miniature photomultiplier. Some of the measurements were taken without the control chambers.

The design of the flat-plate spark chamber is shown in fig. 2a. Its body consists of a glass cylinder 120 mm in diameter with walls 6 mm thick, the end faces of which are ground. The cylinder is held tightly between two solid plates by means of Ø 30 mm textolite pins: no glue or cement is used, and the plates are separated from the cylinder by Teflon seals. The input windows are hermetically sealed by means of 50 μm gauge aluminium foil. The Ø 50 mm electrodes are made from 12 μm gauge aluminium foil wound tightly on to pins. The interelectrode gap is adjusted to 10 μm accuracy (required accuracy $\pm$ 100 μm) by screws which compress springs on the Teflon supports, and it is checked by means of gauge blocks. This type of spark chamber has a capacitance of $\sim$ 30 pF.

Fig. 2b shows a wire spark chamber, the design of which differs in many respects from that described above. The radioactive electron source and a collimator are attached to one of the end plates to form an internal source. A tight fit between the glass cylinder and the Dural end plates is achieved by means of cement consisting of bees' wax (80%) and GOST 9645-61 "Ramzaj" vacuum grease (20%) which has good vacuum properties. The difference between the external pressure and the pressure inside the chamber ($P \leqslant 0.6$ atm) makes the system mechanically stable.

The spark chamber has three wire electrodes consisting of brass rings with a cut-out along their outside radius. A 90 μm gauge beryllium bronze wire is wound over the cut-outs with a pitch of 1.0 or 0.5 mm and soldered. The distance between the wire electrodes is maintained by means of Teflon rings (10 ± 0.01) mm thick in which windows are made beside the central electrode so that the discharge can be observed. The spark chamber may operate both in the three-electrode mode (the plus being transmitted to the central electrode) and in the two-electrode mode (using the central and one of the outer electrodes).

The presence of small admixtures in the gas may considerably alter the spark chamber's efficiency owing to secondary processes. In order to keep the gas pure, after every 10 minutes of measurements it is automatically passed through a purifier filled with calcium chips heated to 700° C. The spark chamber's efficiency thus remains satisfactorily stable. During some of the experiments, when the gas was not cleaned, the efficiency increased with time. The chamber was therefore refilled after every $\sim 10^3$ triggers.

3. Properties of low-pressure spark chambers

3.1. Flat-plate spark chamber

The spark chamber was designed to operate in a mode where the dependence of its efficiency on the parameters of the HV-pulse (pulse-height U and decay time τ) and on the measurement repetition rate (interlock time t_d) was at a flat top. The measurements were carried out at $\tau = RC = 0.35$ μsec ($C = 100$ pF) without a clearing field. Owing to the long dead time of the low-pressure spark chamber (16), the interlock time was set at $t_d \geqslant 2.5$ sec.

The dependence of the spark chamber's efficiency on the height of the HV-pulse features a characteristic gently sloping region-flat top, fig. 3. The slight rise in the flat top is due to the fact that l_e decreases as U increases. The $\eta(U)$ dependence

measured in helium goes higher than it should according to Reter's condition $\alpha (E/P)\, \ell_e \simeq 20$, because the spark chamber's efficiency is measured independent of the positioning of the electron trajectory. In this case the efficiency is affected by the photoeffect from the cathode which is caused by photons originating from showers where the electrons amount to less than the critical number (17). In neon and argon the $\eta (U)$ value is less than that derived from Reter's condition owing to the considerable diffusion of electrons on to the chamber electrodes. Owing to the difference of ℓ and ℓ_e , the dependence of efficiency on gas pressure (fig. 4) is rather different from that to be deduced from calculations of primary specific ionization in He, Ne and Ar. As the gas pressure decreases, the absorption path of the photons released by the discharge plazma lengthens, and a bright halo occurs around the spark. At even lower pressures ($P_{He} \lesssim 0.25$ atm; $P_{Ne} \lesssim 0.10$ atm; $P_{Ar} \lesssim 0.05$ atm) the discharge assumes a diffusive appearance.

The primary ionization measured without the clearing field decreases as the delay time t_d increases owing to the diffusion of electrons on to the electrodes and also owing to adhesion when there are electronegative admixtures in the gas. Diffusion on to the electrodes considerably distorts the results of primary ionization measurements in neon and argon, fig. 5.

3.2. Spark chamber with wire electrodes

The use of wire electrodes increases the spark chamber's efficiency because the diffusion of electrons from the interelectrode gap is compensated by the backward diffusion of electrons produced by a particle ouside the gap. The drifting of electrons on the leading edge of the HV-pulse is also virtually eliminated owing to the very strong electric field near the wire, ($E \simeq 40$ kV/cm at $U = 10$ kV and a wire diameter of ~ 0.1 mm) which leads to the occurence of a discharge in the gas whatever the point where the electron is produced.

Fig. 3 sets out the results obtained from the measurement of the efficiency of low-pressure wire spark chambers, (τ = 0.18 μsec. t_σ = 5 sec). The gas was kept pure during these experiments by periodically refilling the chambers. Fig. 3 shows that in chambers with one (anode) or two wire electrodes the efficiency flat top is higher than in chambers with solid flat electrodes although it is not as long.

4. Primary ionization measurements

In the experiment with control spark chambers the efficiency was determined according to the ratio of the number N_{123} of simultaneous discharges in all three chambers to the number of simultaneous discharges $N = N_{1,2}$ in the two control chambers

$$\eta_{meas} = N_{123} / N , \qquad (6)$$

and in the experiment without control chambers according to the ratio of the number of discharges in the spark chamber to the number of triggers by the scintillation counters

$$\eta_{meas} = N_{\&} / N . \qquad (7)$$

After each run the background recording efficiency was determined. The test spark chamber was triggered from the pulse generator, and the frequency of the discharges generated by random coincidences of the HV-pulse with the β source ionization was recorded. The η_b value varied from 0.02 to 0.06 depending on the source intensity. The true efficiency in the case of a statistically independent background is

$$\eta = \frac{\eta_{meas} - \eta_b}{1 - \eta_b} , \qquad (8)$$

whence it is possible to find the corresponding primary ionization value using (4).

The results from the measurement of primary ionization in terms of the flat-plate spark chamber's efficiency must be corrected for electron diffusion and drift out of the interelectrode gap. As is shown in the Appendix, the diffusion correction is a linear extrapolation of the dependence of the primary ionization measurements on the square root of the effective delay time $t'_d = (t_d + t_o)$ at point $t'_d = 0$, fig. 5, and the t_o value and t_d range where this extrapolation holds depend on the experimental conditions. By replacing t_d by t'_d, the difference between the diffusion of thermalizing electrons and thermal diffusion is taken into account. A correction for electron drift may be made by introducing the effective length l_e of the interelectrode gap. If the discharge begins to develop in the spark chamber on the linear part of the HV-pulse's leading edge, then as is shown in the Appendix

$$l_e = l(1 - KPl/U), \tag{9}$$

where K = const. Consequently, the primary ionization measurements prove to be a linear function of Pl/U, and this is confirmed in the experiment, fig. 6. By extrapolating this dependence to a point where $Pl/U = 0$, we obtain a (dn/dx) value corrected for the drift of electrons to the anode.

It is easy to see that, when there is slight adhesion to the electronegative admixtures, the primary ionization measurements exhibit a linear dependence on the HV-pulse's delay time. This correction is usually much less than the correction for diffusion and was introduced only in the helium experiments where the gas was not purified.

Table 2 sets out the preliminary results obtained from the measurement of primary specific ionization produced by 1.7 - 2.2 MeV relativistic electrons in helium, neon and argon, using low-pressure spark chambers. In Table 3 these measurements are compared with other experimental data on primary specific ionization and with the theoretical calculations.

The following conclusions may be drawn from the results:

1. The measured values of primary specific ionization in helium, neon and argon are in agreement with the theoretical predictions and data from other experiments. This proves that it is possible to measure primary specific ionization in terms of a spark chamber's efficiency.

2. The primary specific ionization measured in a flat-plate spark chamber proves to be lower than that determined by other methods. However, by making corrections for electron diffusion and drift in the interelectrode gap, it is possible to obtain values which are close to the expected values. These corrections amount to $\sim$ 6%, $\sim$ 27% and $\sim$ 25% in He, Ne and Ar respectively.

3. The measurements in wire spark chambers produce primary specific ionization values which are very close to the theoretical predictions and also to results from other experiments owing to the considerable reduction in the effect of diffusion and the drifting of electrons from the interelectrode gap. As a result of this property, the wire spark chamber can be used to measure primary specific ionization even when the gas has a high electron diffusion coefficient. The authors will be publishing separately the final results of their measurements of primary specific ionization in rare gases using a low-pressure wire spark chamber and a continuous gas purification system.

The authors are grateful to A.I. Alikhanyan, an associate member of the USSR Academy of Sciences, for his help with this report, to L.P. Kuzinaya and V.A. Il'in for taking part in the initial stage of the project and also to K.I. Vasil'eva and G.Sh. Kitoshvili who helped to prepare the report for printing. The authors also wish to take this opportunity to thank M.M. Veremeev and A.M. Rogozhin for their useful advice on the construction of the gas purification system.

APPENDIX

1. Electron diffusion during the HV-pulse delay time

If the electron's thermalization time t_τ is less than the HV-pulse's minimum delay $t_{d,\,min} \simeq 0.2$ μsec, the rms shift of an electron σ due to diffusion at times $t > t_{d,min}$ is the same as if the diffusion had been thermal but had begun during time t_0 prior to the passage of the particle (fig. 7a), i.e.

$$\sigma_{t_d > t_{d\,min}} = \sqrt{2D(t_d + t_0)}. \qquad (10)$$

D is the thermal diffusion coefficient and

$$t_0 = \frac{\sigma_{t_d}^2}{2D} - t_d \qquad (11)$$

and the $\sigma^2(t_d)$ dependence may be calculated using the formulae in paper (18)*. If $t_\tau > t_{d,\,min}$ relations (10) and (11) still hold for the limited range of t_d values, but the diffusion coefficient D may be considered to be only approximately constant, and it differs from the thermal diffusion coefficient (figs. 7b and 7c).

Let us now consider the one-dimensional problem of the diffusion of an electron produced at point x_0 in the interelectrode gap on the chamber electrodes at D = const. The density of the probability of an electron at point x at time t is described by the equation

$$\frac{\partial u(x,t)}{\partial t} = D\,\frac{\partial^2 u(x,t)}{\partial x^2}, \quad 0 < x < \ell, \qquad (12)$$

with the following initial and boundary conditions respectively,

---

* In the formulae for t_τ and σ_t^2 in paper (18), the total length of the electron's mean free path must be replaced by the transport mean free path.

$$u(x,0) = \delta(x - x_0),$$
$$u(0,t) = u(\ell,t) = 0. \qquad (13)$$

By considering only times that are so short that $\sqrt{Dt}/\ell \ll 1$ (semi-infinite two- dimensional problem), we find the probability $\alpha(x_0, t)$ of an electron produced at point x_0 hitting the chamber electrodes

$$\alpha(x_0,t) = 1 - \Phi\left(\frac{x_0}{2\sqrt{Dt}}\right) \qquad (14)$$

where

$$\Phi(y) = \frac{2}{\sqrt{\pi}} \int_0^y e^{-z^2} dz$$

Let $P_j = n^j e^{-n}/j!$ - the probability of j primary electrons appearing in the interelectrode gap and W_k is the probability of k secondary electrons being produced by a primary. By averaging $\alpha(x_0 t)$ in terms of x_0 and allowing for the fact that for a certain number of events all the secondary electrons may hit the electrodes owing to diffusion, thus reducing the chamber's efficiency, we obtain

$$1 - \eta = P_0 + \sum_{j=1}^{\infty} P_j \left[\sum_{k=1} W_k \frac{1}{\ell} \int_0^{\ell} \alpha^k(x_0,t)\, dx_0\right]^j =$$
$$= P_0 + \sum_{j=1}^{\infty} P_j \alpha^j(t) = e^{-n[1-\alpha(t)]}, \qquad (15)$$

where

$$\alpha(t) = \sum_{k=1}^{\infty} \alpha_k(t) = \sum_{k=1}^{\infty} \frac{W_k}{\ell} \int_0^{\ell} \alpha^k(x_0,t)\, dx_0 \qquad (16)$$

is the mean probability of all the secondary electrons produced by one primary electron hitting the chamber electrodes as a result of diffusion.

We may go further by writing

$$\alpha_k(t) = \frac{W_k}{\ell} \cdot 2\sqrt{Dt} \int_0^{\ell/2\sqrt{Dt}} \left[1 - \Phi\left(\frac{x_0}{2\sqrt{Dt}}\right)\right]^k d\left(\frac{x_0}{2\sqrt{Dt}}\right) = W_k \frac{2\sqrt{Dt}}{\ell} C_k \qquad (17)$$

and as $\ell / 2\sqrt{Dt} \gg 1$, therefore C_k = const.
Hence

$$\alpha(t) = \frac{2\sqrt{Dt}}{\ell} \sum_{k=1}^{\infty} W_k C_k = \text{const} \cdot \sqrt{Dt} . \qquad (18)$$

By substituting $(t_d + t_o)$ for t, we finally obtain

$$n[1-\alpha(t)] = n(1-\text{const}\sqrt{t_d+t_o}) = \frac{273}{T} p\varrho \frac{dn}{dx}(1-\text{const}\sqrt{t_d+t_o}) . \qquad (19)$$

2. Electron drift in the HV-pulse field

In a low-pressure spark chamber filled with pure rare gas photons from a shower of electrons amounting to less than the critical number may cause a discharge owing to the photoeffect from the cathode. Therefore, the effective length of the interelectrode gap is shortened only by the drift of electrons in the HV-pulse field before they are multiplied. In order to produce a shower, an accelerated electron must gather the energy required to ionize the gas atoms: this energy corresponds to a particular electric field value E_i and time t_i from the instant when the HV-pulse is transmitted. Assuming that the shower begins to develop on the linear part of the HV-pulse's leading edge, fig. 8, we find that the electron shift during time t_i is

$$d_i = \int_0^{t_i} v(E/p)\,dt = t_b \frac{p\ell}{U} \int_0^{E_i/p} v(E/p)\,d(E/p) = k\frac{p\ell}{U} . \qquad (20)$$

Here $v(E/p)$ is the electron's rate of drift, t_f is the length of the pulse's leading edge (fig. 8) and k = const. Hence

$$\ell_e = \ell - d_i = \ell\left(1 - k\frac{p}{U}\right) \qquad (21)$$

Table 1

Gas under investigation	Calculated primary specific ionization at P = 1 atm, t^o = 0° C (14) γ = 4	Gas pressure P atm in chamber at t^o = 20° C corresponding to an efficiency of η = 0.8 (l = 1 cm)
He	3.5 (3.79*)	0.47 (0.45*)
Ne	11.4	0.15
Ar	25.8	0.07
Kr	35.4	0.049
Xe	48.1	0.036

* Allowing for additional ionization caused by the production of molecular ions of rare gas by excited atoms.

Table 2

	Gas under investigation	Pressure P atm	Electrode design ⊕	Electrode design ⊖	Interelectrode gap, l, mm	Primary specific ionization under normal conditions $(dn/dx)\,cm^{-1}$	Method of gas purification
1	He	0.4	fl.	fl.	10 ± 0.01	3.43 ± 0.08	Circulated through calcium purifier
2			w*.	w*.	18.8 ± 0.1	3.71 ± 0.11	Refilling
3			w*.	w*.	10.0 ± 0.1	3.70 ± 0.13	"
4			w*.	w**.	10.0 ± 0.1	3.78 ± 0.09	"
5			w*.	w**.	10.0 ± 0.1	3.66 ± 0.09	"
6		0.6	fl.	fl.	10.0 ± 0.01	3.45 ± 0.08	Circulated through calcium purifier
7			fl.	w*.	10.7 ± 0.05	3.61 ± 0.39	Refilling
8			w*.	fl.	10.7 ± 0.05	3.60 ± 0.06	"
9			w*.	w*.	10.0 ± 0.1	3.67 ± 0.12	"
10			w*.	w**.	10.0 ± 0.1	3.61 ± 0.11	"
11	Ne	0.15	fl.	fl.	10.0 ± 0.01	10.59 ± 0.56	"
12			w*.	w*.	10.0 ± 0.1	11.1[illegible] ± [illegible].22	"
13	Ar	0.10	fl.	fl.	10.0 ± 0.01	27.0 ± 1.8	"
14			w*.	w*.	10.0 ± 0.1	27.1 ± 0.9	"

fl. - flat electrode, w. - wire electrode
* - Distance between wires d = 1 mm

Table 3

Gas under investigation	Experimental method	Minimum primary specific ionization under normal conditions (dn/dx) cm^{-1}	
		Experiment	Theory (13,14)
He	Low-efficiency counter (5)	5.02 ± 0.06	3.50
	Streamer chamber (11)	3.83 ± 0.11	(3.78**)
	Low-pressure spark chamber	3.44 ± 0.06 3.66 ± 0.06*	
Ne	Low-efficiency counter (5)	12.4 ± 0.13	11.4
	Low-pressure spark chamber	11.10 ± 0.22	
Ar	Low-efficiency counter (5)	27.8 ± 0.31	25.8
	Wilson chamber (6)	28.6 ± 0.5	
	Diffusion chamber (7)	26.4 ± 1.8	
	Low-pressure spark chamber	27.1 ± 0.9	

* Chemically pure gas circulating through hot calcium.

** Allowing for additional ionization caused by the production of molecular ions by excited atoms.

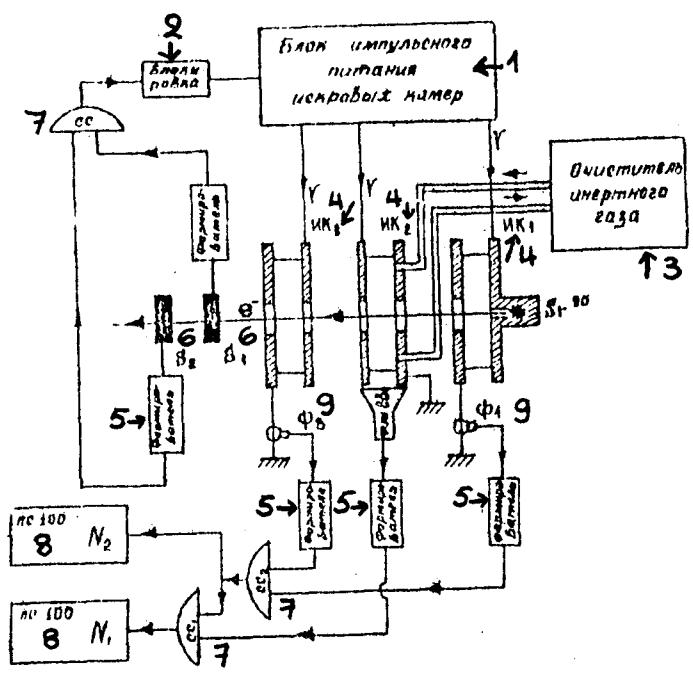

Fig. 1 Layout of one type of experimental device.

1. Pulsed power supply for spark chambers.
2. Interlock.
3. Inert gas purifier.
4. Spark chamber.
5. Shaper.
6. Scintillation counter.
7. Coincidence circuit.
8. Scaling circuit.
9. Ferrite rings.

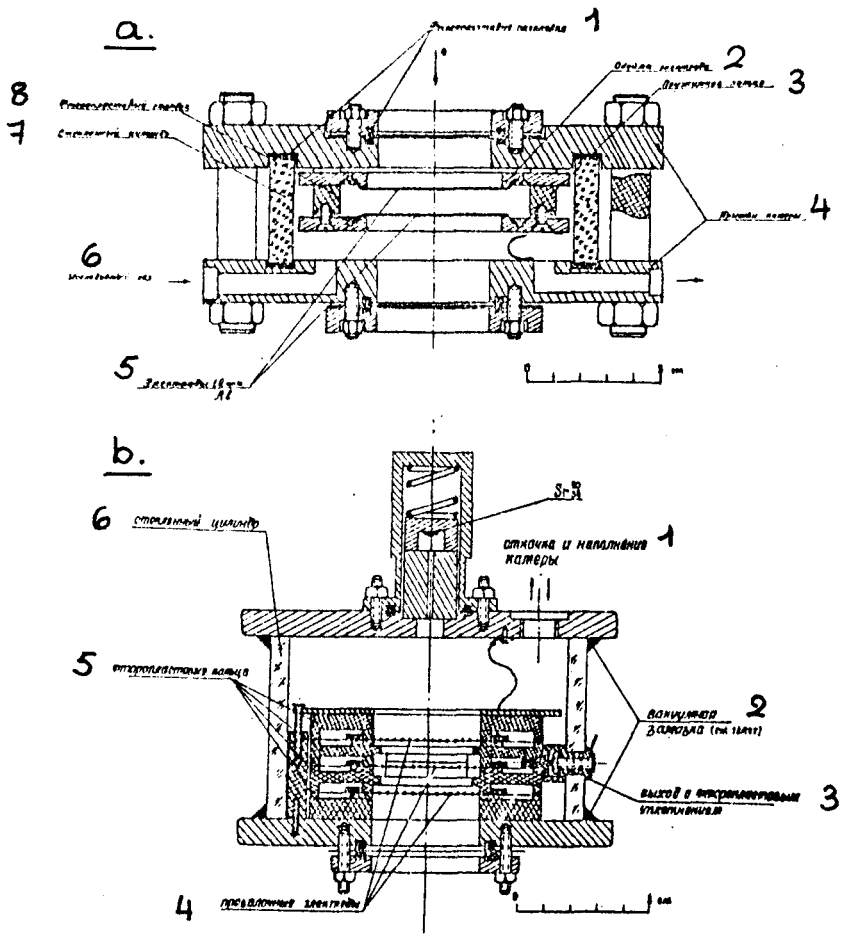

Fig. 2 Design of low-pressure spark chamber

a) with flat electrodes;
b) with wire electrodes.

Key to figure 2a

1. Teflon seals.
2. Electrode holder.
3. Ring clamp.
4. Chamber end plates.
5. Aluminium electrodes.
6. Gas under investigation.
7. Glass cylinder.
8. Teflon support.

Key to figure 2b

1. Inlet and outlet.
2. Vacuum grease (see text).
3. Output with Teflon seal.
4. Wire electrodes.
5. Teflon rings.
6. Glass cylinder.

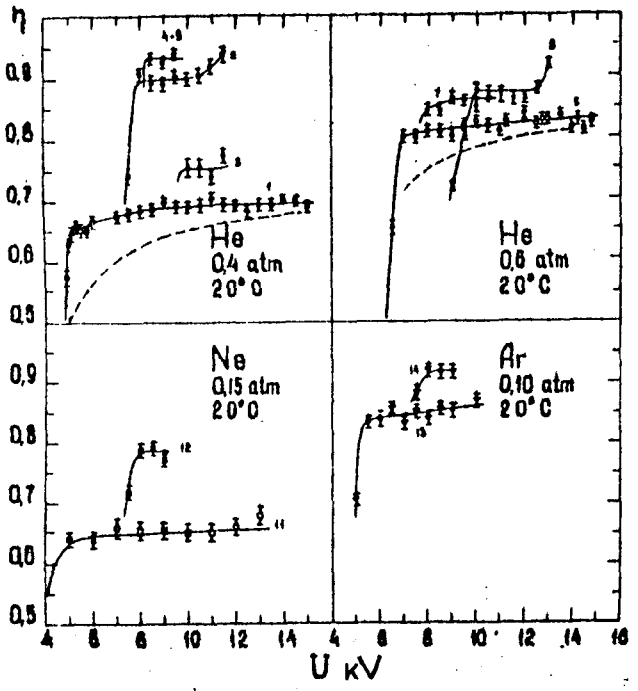

Fig. 3 Dependence of a low-pressure spark chamber's efficiency on the height U of an HV-pulse (t_d = 0.20 - 0.25 μsec). Experimental data: ●, ■, ▼, × - wire spark chambers; ○, □, ▽ - flat-plate spark chambers. Plots 1 and 6 were obtained using a purification system: for the remainder the gas was renewed periodically. The solid lines are drawn through the experimental points for convenience, and the dotted lines correspond to the Reter condition αl_e = 20. The numbers beside the plots correspond to the numbers of experiments in Table 2.

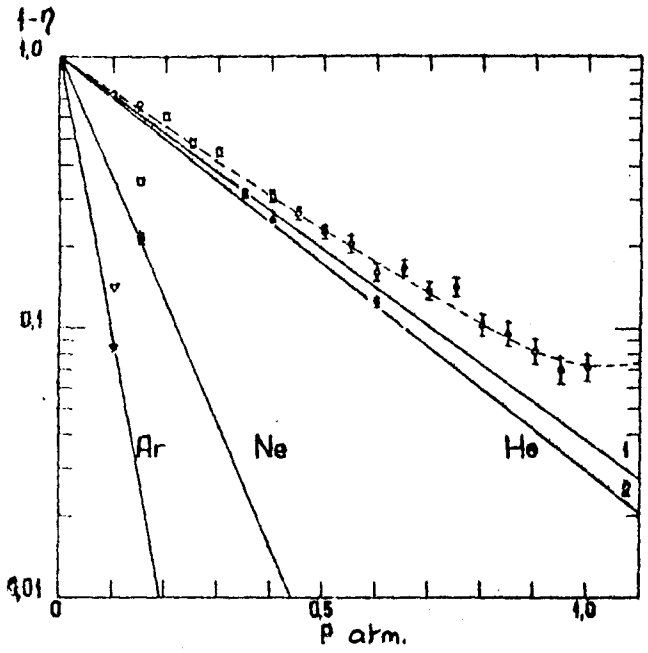

Fig. 4 Dependence of a spark chamber's inefficiency on gas pressure. Experimental data: ○ , □ , ▽ - in flat-plate spark chambers; ● , ■ , ▼ - in wire spark chambers. The solid lines correspond to the dependences calculated on the basis of the minimum primary specific ionization values under normal conditions taken from Table 1. Plots 1 and 2 correspond to the values $(dn/dx)^{He}_{min}$ = 3.5 and 3.79 respectively. The hatched line corresponds to plot (1) corrected for diffusion and electron drift away from the interelectrode gap.

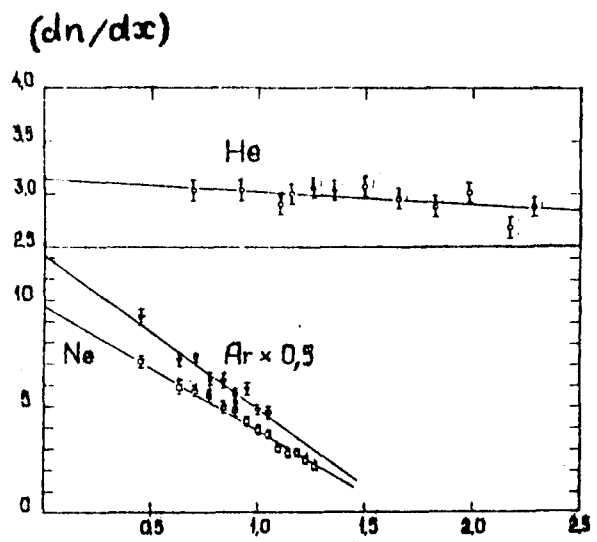

Fig. 5 Measurement of primary ionization in He, Ne and Ar in a flat-plate spark chamber as a function of the HV-pulse delay time, (t = 20° C). The data are reduced to 1 atm. The approximated straight lines are drawn by the least squares' method.

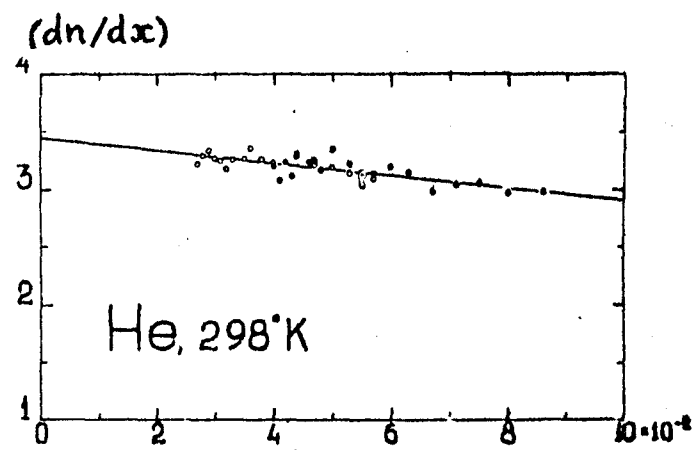

Fig. 6 Measurement of primary ionization in a flat-plate helium spark chamber as a function of $P\ell / U$. ○ - P = 0.4 atm; ● - P = 0.6 atm. The approximated straight line is drawn by the least squares' method.

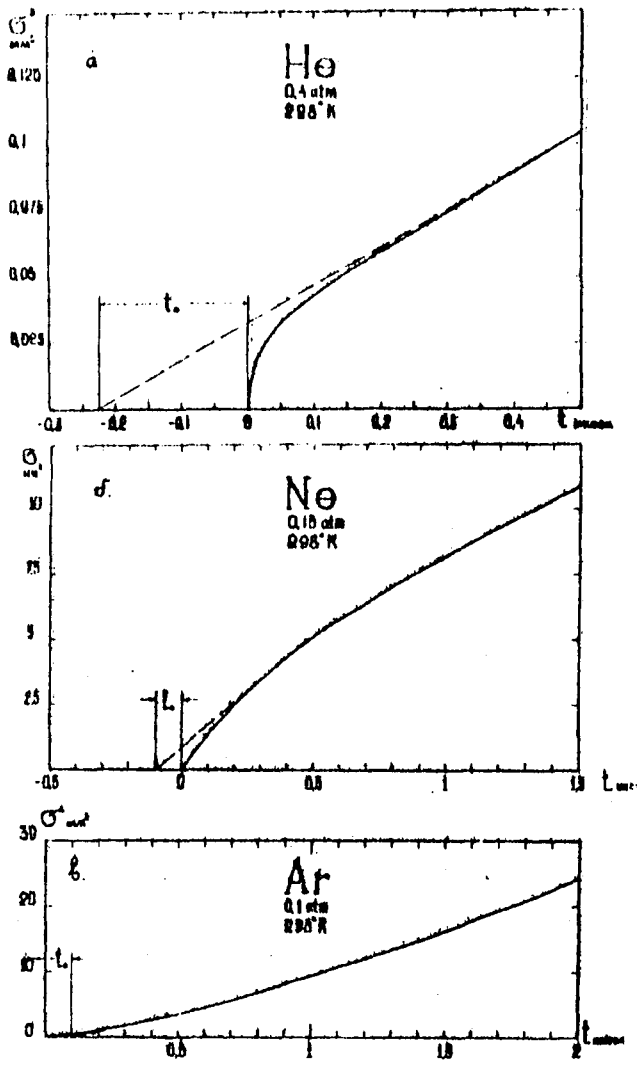

Fig. 7 Figures for deriving the dependence of a flat-plate spark chamber's efficiency on the HV-pulse delay time.

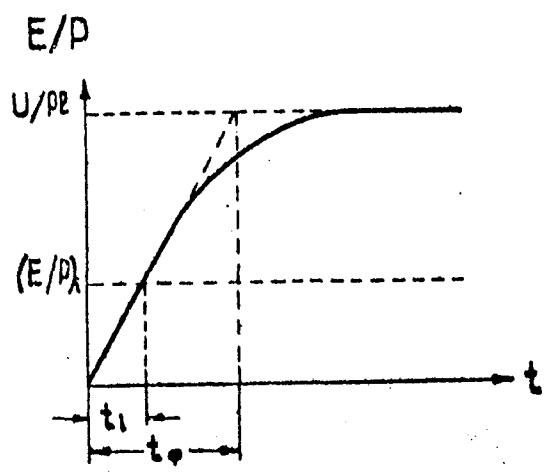

Fig. 8 Figure for deriving the (E/P) dependence of a flat-plate spark chamber's efficiency.

Bibliography

1. M.I. Dajon, Yu.A. Leksin, UFN 80, 281, (1963).
2. G.I. Merzon, "Experimental programme at the 1000 GeV cybernetic accelerator", publ. USSR Academy of Sciences Electronics Institute, p.95 (1967).
3. A.A. Tyapkin, JINR Preprint, I-3686, (1968).
4. F.L. Hereford, Phys. Rev., 74, 574 (1948).
5. G.W. McClure, Phys. Rev., 90, 796, (1953).
6. R. Decker, H. Kullenkampf, Z. Phys., 137, 638 (1954).
7. L. Wiedecke, Z. Phys., 154, 150, (1959).
8. V.V. Bovin, P.A. Krupchitskij, I.I. Pershin, B.V. Chirikov. PTE N° 3, 19, (1957).
9. E. Gygi, F. Schneider, CERN Rep. 66-14 (1966).
10. V.A. Davidenko, B.A. Dolgoshein, S.V. Somov. ZhETF 55, 426 (1968).
11. V.A. Davidenko, B.A. Dolgoshein, S.V. Somov. ZhETF 56, 3 (1969).
12. V.A. Davidenko, B.A. Dolgoshein, S.V. Somov, V.I. Starosel'tsev. ZhETF 58, 130 (1970).
13. V.K. Ermilova, L.P. Kotenko, G.I. Merzon, V.A. Chechin. ZhETF 56, 1608 (1969).
14. V.K. Ermilova, L.P. Kotenko, G.I. Merzon, V.A. Chechin. FIAN Preprint N° 152, Moscow, 1969.
15. M.F. Lomanov, B.V. Chirikov. PTE N° 5, 22 (1957).
16. T. Bunaciu, S. Kullander. NIM 58, 173 (1968).
17. M.I. Dajon, B.A. Dolgoshein, V.I. Efremenko, G.A. Leksin, V.A. Lyubimov. "Spark chamber", Atomizdat, 1967.
18. V.A. Davidenko, B.A. Dolgoshein, S.V. Somov, V.N. Starosel'tsev. ZhETF 57, 84 (1969).

****